Brain-inspired Sensorimotor Robotic Platform
Learning in Cerebellum-driven Movement Tasks through a Cerebellar Realistic Model

Claudia Casellato[1], Jesus A. Garrido[2,3], Cristina Franchin[1], Giancarlo Ferrigno[1], Egidio D'Angelo[2,4] and Alessandra Pedrocchi[1]

[1]*Politecnico di Milano, Dept of Electronics, Information and Bioengineering, Via G. Colombo 40, 20133 Milano, Italy*
[2]*University of Pavia, Dept of Brain and Behavioral Sciences, Neurophysiology Unit, Via Forlanini 6, I-27100 Pavia, Italy*
[3]*Consorzio Interuniversitario per le Scienze Fisiche della Materia (CNISM), Via Forlanini 6, I-27100 Pavia, Italy*
[4]*IRCCS, Istituto Neurologico Nazionale C. Mondino, Brain Connectivity Center, Via Mondino 2, Pavia, I-27100, Italy*

Keywords: Cerebellum, Learning, Vestibular-Ocular Reflex, Plasticity.

Abstract: Biologically inspired neural mechanisms, coupling internal models and adaptive modules, can be an effective way of constructing a control system that exhibits a human-like behaviour. A brain-inspired controller has been developed, embedding a cerebellum-like adaptive module based on neurophysiological plasticity mechanisms. It has been tested as controller of an ad-hoc developed neurorobot, integrating a 3 degrees of freedom serial robotic arm with a motion tracking system. The learning skills have been tried out, designing a vestibular-ocular reflex (VOR) protocol. One robot joint was used to get the desired head turn, while another joint displacement corresponded to the eye motion, which was controlled by the cerebellar model output, used as joint torque. Along task repetitions, the cerebellum was able to produce an anticipatory eye displacement, which accurately compensated the head turn in order to keep on fixing the environmental object. Multiple tests have been implemented, pairing different head turn with object motion. The gaze error and the cerebellum output were quantified. The VOR was accurately tuned thanks to the cerebellum plasticity. The next steps will include the activation of multiple plasticity sites evaluating the real platform behaviour in different sensorimotor tasks.

1 INTRODUCTION

Biologically inspired neural mechanisms can be an effective way of constructing a control system that exhibits a human-like behavior. In the framework of distributed motor control, connecting brain-inspired kinematic and dynamic models, human-like movement planning strategies and adaptive neural systems inside the same controller is a very challenging approach, bridging neuroscience and robotics.

Motor learning is obviously necessary for complicated movements such as playing the piano, but it is also important for calibrating simple movements like reflexes, as parameters of the body and environment change over time. Cerebellum-dependent learning is demonstrated in different contexts (Boyden et al., 2004; van der Smagt, 2000), such as multiple forms of associative learning, where the learning is based on the stimulus-response association. Eye blinking conditioning, saccadic eye movements, vestibular ocular reflex and reaching arm movements are well-known examples of these mechanisms (Donchin et al., 2012).

The Marr-Albus and Ito models propose that changes in the strengths of parallel fiber–Purkinje cell synapses could store stimulus-response associations by linking inputs with appropriate motor outputs, following a Hebbian learning approach. Error-based learning and predictive outputs are working principles of these cerebellum models (Marr, 1969; Albus, 1971; Ito, 2006).

We have built up a real human-like sensorimotor platform with cerebellar-like learning skills. The sensory systems are integrated, monitoring the environment and the muscular-skeletal system state. Based on the neurophysiology of the distributed neuromotor control system, the robotic control has

Casellato C., A. Garrido J., Franchin C., Ferrigno G., D'Angelo E. and Pedrocchi A..
Brain-inspired Sensorimotor Robotic Platform - Learning in Cerebellum-driven Movement Tasks through a Cerebellar Realistic Model.
DOI: 10.5220/0004659305680573
In *Proceedings of the 5th International Joint Conference on Computational Intelligence* (SSCN-2013), pages 568-573
ISBN: 978-989-8565-77-8

been designed as a real-time coupling of multiple neuronal structures and mechanisms; the cerebellum model, based on the plasticity principles ascribed to the synapses between parallel fibers and Purkinje cells, is expected to learn throughout the task repetitions (Casellato et al., 2012).

One protocol stressing the cerebellum role has been designed and implemented: the vestibular-ocular reflex (VOR). The VOR produces eye movements which aim at stabilizing images on the retina during head movement. The VOR tuning is ascribed mainly to the cerebellum loop, in particular to the cerebellar flocculus which creates an inhibitory loop in the VOR circuit. There are a lot of evidences of its role from lesions, pharmacological inactivation and genetic disruption studies (Burdess, 1996). The learning is based on the temporal association of the two stimuli, head turn and motion of retinal image, i.e. the system learns that one stimulus will be followed by another stimulus and a consequent predictive compensatory response is gradually produced and accurately tuned.

2 METHODS

2.1 Robotic Platform

A flexible, not cumbersome and manoeuvrable robotic platform has been built and its controller has been developed in Visual C++.

The main robot is a Phantom Premium 1.0 (SensAble™), with 3 rotational Degrees of Freedom (DoFs). It is equipped with digital encoders at each joint and it can be controlled with force and torque commands. It connects to the PC via the parallel port interface. It is integrated with a motion capture device, a VICRA-Polaris (NDI™), which is an optical measurement system acquiring marker-tools at 20 Hz. Another robotic device (Phantom Omni, SensAble™) is included into the platform so as to impose object motion during the protocol performance. The controller has been developed exploiting the OpenHaptics toolkit (SensAble™) and the Image-Guided Surgery Toolkit (IGSTK).

The robotic DoFs are controlled through torque signals, by exploiting the low-level access provided by the Haptic Device Application Programming Interface (HDAPI). For stability, this control loop must be executed at a consistent 1 kHz rate; in order to maintain such a high update rate, the servo loop is executed in a separate, high-priority thread (HDCALLBACKS). For the motion tracking system integration, the IGSTK low-level libraries (http://www.igstk.org/), whose architecture is based on Request-Observer-pattern, are used. Each desired tool is identified by a .rom file, which defines the unique geometry of the reflective markers composing the tool itself.

In our configuration, wireless passive tools have been placed in correspondence of the robotic end-effector (gaze) and of the objects of interest in the environment. An a-priori calibration procedure allows to identify the constant roto-translation between the reference system of the tracking device (Visual system) and of the robot (Proprioceptive system), thus it represents a Body/Eye calibration.

2.2 Cerebellum Model

The cerebellar system hereby implemented and embedded into the whole control system is based on the model proposed in (Garrido et al., submitted). It takes into account the major functional hypotheses that each cerebellar layer endows, modeling Mossy Fibers (MF), GRanular layer (GR), Purkinje Cell layer (PC) and Deep Cerebellar Nuclei (DCN). These cerebellar layers have been interconnected, as shown in Figure 1, where PF (Parallel Fibers) are the axons of GR cells and the CF are the Climbing Fibers coming from the Inferior Olive (IO). This model implements three plasticity mechanisms at different synapses: PF→PC (w), PC→DCN (b) and MF→DCN (v). In previous models, the GR layer has been suggested to generate non-recurrent states after the stimulus onset in eyeblink-conditioning tasks (Yamazaki and Tanaka, 2007). The large number of granular cells (and then of their axons, i.e. PF) guarantees a reliable pattern separation, which means that similar input patterns would be sparsely re-encoded into largely not-overlapping populations of GR activity. Climbing fibers carry the error signal, generating complex spikes on PC. A state-error correlator emulates the Purkinje cell operability, driving the PF→PC long-term plasticity.

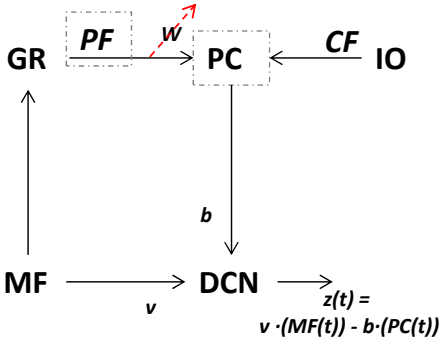

Figure 1: Scheme of the cerebellar network.

Finally, an adder/subtractor module receives the inputs coming from the mossy fibers (multiplied by the MF→DCN synaptic weight *v*) and subtracts the signal coming from the cerebellar cortex (multiplied by its own synaptic weight *b*). Indeed, the MF→DCN connections are excitatory, while the PC→DCN ones are inhibitory. In the cerebellum model used in this work (Figure 1), only one plasticity site was taken into account: the long-term depression (LTD) and long-term potentiation (LTP) at cerebellar cortex (PF→PC); thus, the PC activity changes along time and along repetitions (PC(t)) depending on the tuneable strength at the synapses with the PF (*w*). The synapses strengths *v* and *b* are set constant equal to 1. Thus, the DCN output is maximum (*z*=1) when the Purkinje cells do not fire (PC(t)=0), i.e. the PF→PC weights are depressed (LTD); whereas the DCN output is minimum (*z*=0) when the Purkinje cells are maximally activated (PC(t)=1), i.e. the PF→PC weights are potentiated (LTP). LTD is driven by CF, in particular it is proportionally induced by the frequency of the generated complex spikes; whereas LTP is constantly produced when an input activity is present but in absence of CF stimulation related to this activity (unsupervised learning). The plasticity rule on *w* is defined as follows:

$$\Delta w_{PF_j \to PC_i}(t) = \begin{cases} \frac{LTP_{max}}{(\varepsilon_i + 1)^{\alpha}} - LTD_{max} \cdot \varepsilon_i & if\ PF_j\ is\ active\ at\ t \\ 0 & otherwise \end{cases}$$

where $\Delta w_{PFj\text{-}PCi}(t)$ represents the weight change between the *j-th* parallel fiber and the target PC associated to the muscle (agonist or antagonist), ε_i is the current activity coming from the associated climbing fiber (which represents the normalized error along the executed head-eye movement), LTP_{max} and LTD_{max} are the maximum LTP and LTD values and α is the LTP decaying factor. LTP_{max} and LTD_{max} are set 0.015 and 0.15 respectively and α = 1000, to avoid early plasticity saturation.

The somatotopic approach is kept at level of IO, PC and DCN: a group of IO carries information about the error (positive and negative separately) of a specific involved DoF and projects on a corresponding group of PC. They themselves project on a corresponding group of DCN, which thus produce an agonist or antagonist motion (positive and negative) for each specific controlled DoF.

2.3 Protocol: VOR

The stimulus is the head turn, which is produced by rapidly imposing a motion to the joint 2 of the robotic device, with a pre-defined joint time-profile, occurring in a head-fixed reference system (fixed robotic reference system). The gaze is defined as the orientation of the second link of the robot, i.e. the one linking joint 2 and joint 3.

The vestibular sensory input is used by the GR layer to generate the system state.

The CF carry the visual error, i.e. the image retinal slip, computed with data from the optical tracking system. Assumed that the goal is to fix an environmental object, this visual error is computed as the disalignment angle with respect to the stable condition before head turn, where the gaze direction and the object center are aligned. Since the acquisition frequency of the tracking system, the retinal slip is more delayed or not strictly synchronized with the faster vestibular information, which is physiologically meaningful.

During the head turn, the only controller acting on joint 3 (compensatory eye turn) is the cerebellum, so as to be fully neurophysiologically plausible. Indeed, since the required rapid reflexive response to compensate for head motion, the inaccurate and delayed feedback cannot be activated. It is worthy to note that the robotic device was used so as to get the two involved joints (joints 2 and 3) moving on a horizontal plane, where the gravity has not to be counterbalanced. The protocol and the set-up are shown in Figure 2.

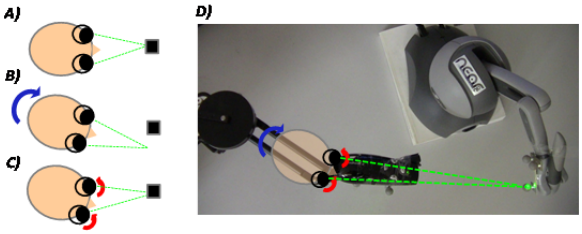

Figure 2: The VOR protocol. A: stable condition. B: head turn leading to an image slip. C: head turn and compensatory eye movement. D: the set-up: Phantom Premium with the optical tool on the end-effector; Phantom Omni with the object-tool. The green laser is attached parallel to the second link (i.e. the gaze direction) to highlight the gaze point on the environmental scene.

In order to quantify the VOR performance, the gain at maximum vestibular stimulus has been computed, as absolute ratio between eye turn and head turn (angles) at the maximum achieved head turn. Different sequences of repetitions were tested, in order to quantify the modulation of VOR with different stimuli presentation.

- *Test 1 –VOR Calibration*

We have designed a sequence of 130 trials. In the first 110 repetitions, a head turn of 22° with respect

to the rest head-tilt was imposed with a speed equal to 5.5°/s (head turn duration = 4 s). During the last 20 trials, the head turn was halved (11°, at 2.75°/s). Each trial lasted 4.5 seconds, thus including a stabilization phase between consecutive trials (0.5 s), where the head turn did not occur. The eye motion was driven only by the cerebellum output (joint 3 torque), with a constant gain equal to 100.

- *Test 2: Head Motion + Object Motion*

The head motion was paired with additive image motion; it means that the image motion was due not only to the head turn but even to the real object displacement (Boyden et al., 2004). We have tested a sequence of 110 trials where the object motion was synchronously added to the head rotation (same onset instant). The head turn was as in Test 1 (22° in 4 seconds). The object, attached to the Phantom Omni, was moved at a speed equal to 4 cm/s. Three conditions were created; the first one was defined as a standard VOR calibration; the second condition with the object moving in the same direction as the head and then the third condition with the object moving in the opposite direction than the head rotation.

3 RESULTS

- *Test 1 – VOR Calibration*

Figure 3 shows the results of these tests.

In the first trials of the task sequence, the VOR is poorly calibrated, thus head movement results in image motion on the retina, which would mean blurred vision. Indeed, in these first trials, the gaze error reaches values higher than 16° when the head is maximally turned. Along task repetitions, the cerebellum-driven motor learning adjusts the VOR to produce more accurate eye motion, thus reducing and stabilizing the gaze error.

In the last 20 trials (2nd condition), where the head rotation amplitude is reduced, the first repetitions are characterized by an eye overcompensation, as learnt during the previous condition; it means that the eyes turn too much with respect to the head motion, overcoming the object. Very rapidly, the VOR is re-tuned, stabilizing back the error at the minimum level. From the zoom at the right-top of the figure, it can be marked that the shape of the gaze error changes between the two conditions, since the onset of the head motion is the same but the head is rotating slower and it reaches a less turn from the initial head-tilt; thus the cerebellum-driven eye motion starts correctly but then it overcompensates the head motion. That is adjusted within few repetitions of this 2nd condition.

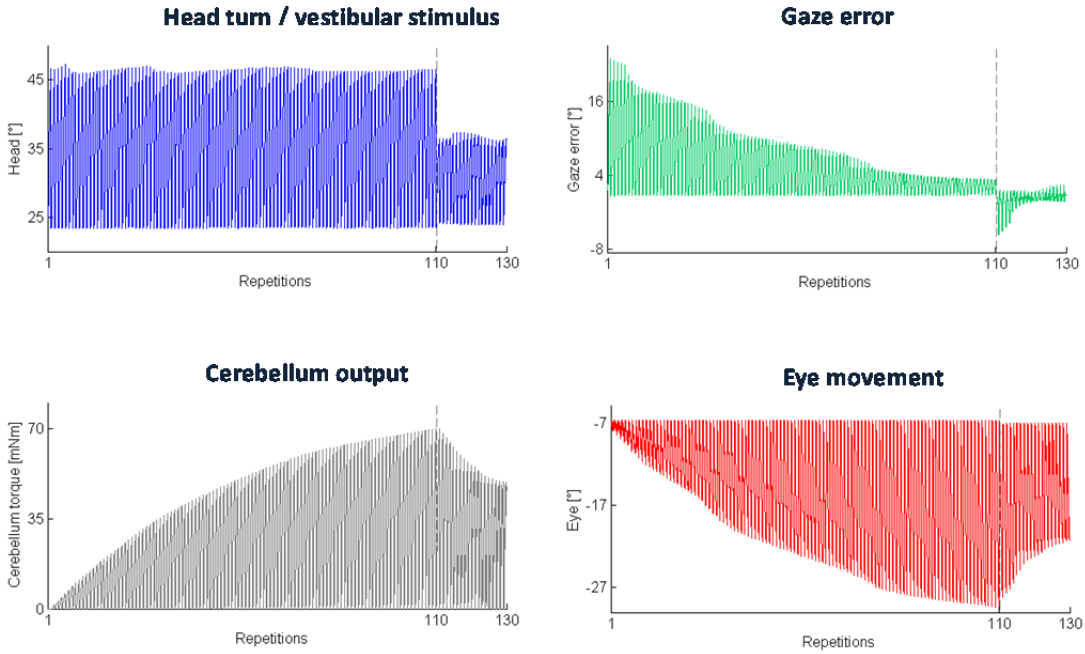

Figure 3: Test 1 – VOR Calibration. Top-left: the actual joint 2; top-right: the gaze error; down-left: the cerebellar output (DCN activity); down-right: the eye movement produced by the cerebellum output.

The cerebellum output (already multiplied to the gain, thus equal to the torque provided to joint 3 actuator) and the produced eye motion increase. Then, in the 2nd condition where the head rotation amplitude is reduced, VOR needs to be decreased; thus, the cerebellar activity is modulated until it reaches an analogous value as at the end of the first condition. The decreasing process is faster than the increasing one.

- *Test 2: Head Motion + Object Motion*

The sequence of 110 trials where the head turn is constant and the object motion, when occurs, starts together with the head motion is depicted in Figure 4. After a VOR calibration compensating only for head turn, the additive object motion represents a gain-down and a gain-up stimulus (2nd and 3rd conditions, respectively). Since, as demonstrated in Test 1, the VOR decreasing is faster, the 2nd condition is made up of less repetitions than 3rd condition.

Figure 5 is focused on the gaze error and the gain parameter, which is tuned during the repetitions in each condition. Unlike Test 1, here the stable gain that is achieved at the end of each condition is not the same; indeed, the object motion induces a modulation of the needed eye motion, even if the head turn has the same amplitude and duration across all conditions. Thus, the gain is modified (gain-down and gain-up).

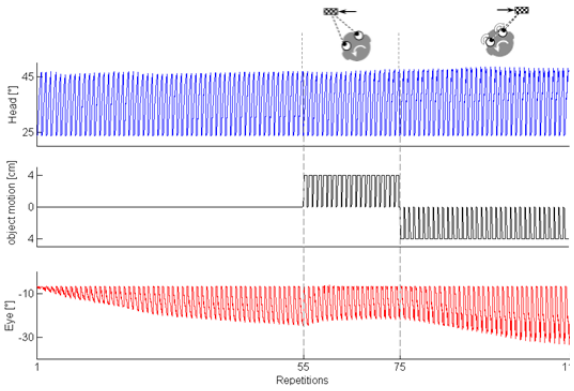

Figure 4: Test 2 - head motion + object motion. The first row shows the head angle; the second row depicts the object movement (by Phantom Omni motion); the third row represents the produced eye compensatory eye movement; in the three conditions: the VOR calibration with fixed object, the VOR gain-down and the gain-up inducing object motion.

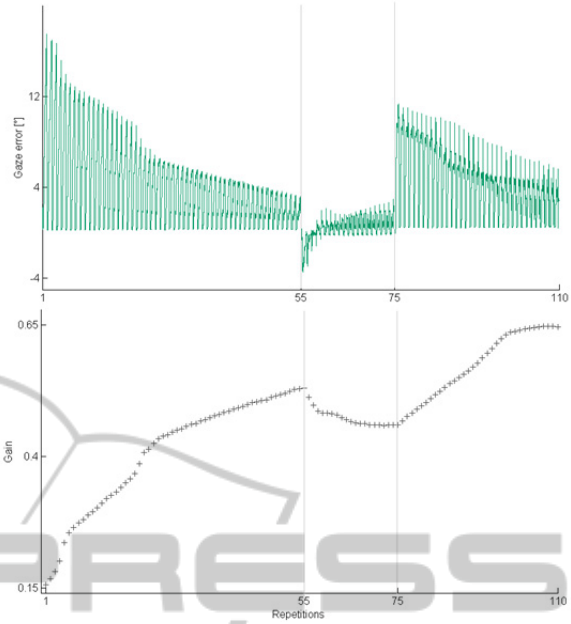

Figure 5: The gaze error and the gain parameter in the task sequence with gain-down and gain-up stimuli.

4 DISCUSSION

The developed integrated robotic platform with its controller is able to neurophysiologically reproduce representative cerebellum-driven motor behaviors. The cerebellar model can be viewed as a "black box" associative memory, whose function is determined by how its inputs and outputs are connected in the system that is embedded in.

The VOR uses a head turn signal sensed by the vestibular system to drive an implicit feedfoward compensation scheme. Purkinje cells activity can properly tune eye movements.

In the first test about VOR calibration, the two conditions in row show a sort of generalization of learning, tuning the VOR response depending on the features of the head turn stimulus. In neurophysiological terms, the generalization process should be based on an overlap of neuronal activations, i.e. neurons active at low vestibular stimuli are a subset of those active at higher stimuli.

The second test highlights the VOR tuning with additive perturbations due to object displacement. We found that the gain-down trials show a faster learning rate than the gain-up trials. This asymmetry is due to the different mechanisms; indeed, since the system was set to inhibit the DCN activity at the start of the learning process, increasing in VOR involves only the LTD mechanism (reduction of PC

activity and thus increase of DCN activity). On the other hand, the need of decreasing VOR and the presence of overcompensation enable simultaneously the reduction of agonist DCN activity (PF-PC LTP) and the increase of antagonist DCN activity (PF-PC LTD). Thus, during the VOR gain-down, the stiffness of the muscle is temporally increased and, after some time, it is reduced to the minimal level.

In summary, a simple model with parallel, sparsely coded channels, and with a single plasticity mechanism that alters a subset of these channels, can go a long way in explaining the general capacity of motor learning in the VOR to exhibit specificity for the particular stimuli present during training. Learning, modulation and extinction proprieties emerge.

According to the plasticity distribution at multiple synaptic sites (Gao et al., 2012), the next steps will be focused on the activation of the other plasticity rules of the cerebellar model, expecting a more stable and more accurate learning. The modulation of these connectivities (MF→DCN and PC→DCN) should lead to a learning generalization, which will be tested through multiple tasks, such as force-field paradigm in multi-joint reaching and associative protocols such as eye blinking classical conditioning task (Hwang and Shadmehr, 2005; Yamamoto et al., 2007; Hoffland et al., 2012). Moreover, for a more realistic computational scenario, the sensorimotor platform will embed the spiking version of this developed multiple-plasticity cerebellar model (Luque et al., 2011).

5 CONCLUSIONS

The developed platform, a real neuro-robot able to interact with the environment in multiple forms, is a flexible and versatile test bed to concretely interpret specific features of functional biological models, in terms of neural connectivity, plasticity mechanisms and functional roles into different closed-loop sensorimotor tasks. In particular, the focus is on the most CNS plastic structure, the cerebellum.

ACKNOWLEDGEMENTS

This work has been supported by the EU grant REALNET (FP7-ICT-270434).

REFERENCES

Albus, J.S. (1971). A Theory of Cerebellar Function. *Math Biosci.,* 10, 25–61.

Boyden, E.S., Katoh, A., Raymond, J.L. (2004). Cerebellum-dependant Learning: The Role of Multiple Plasticity Mechanisms. *Annu Rev Neurosci.*, 27, 581–609.

Burdess, C. (1996). The Vestibulo-Ocular Reflex: Computation in The Cerebellar Flocculus. Retrieved (n.d.) from hxxp://bluezoo.org/vor/vor.pdf.

Casellato, C., Pedrocchi, A., Garrido, J.A., Luque, N.R., Ferrigno, G., D'Angelo, E., Ros, A. (2012). An Integrated Motor Control Loop of a Human-like Robotic Arm: Feedforward, Feedback and Cerebellum-based Learning. *Biomedical Robotics and Biomechatronics (BioRob), 2012 June 24-27 4th IEEE RAS & EMBS International Conference,* no., 562-567. doi: 10.1109/BioRob.2012.6290791.

Donchin, O., Rabe, K., Diedrichsen, J., Schoch, B., Gizewski, E.R., Timmann, D. (2012). Cerebellar Regions Involved in Adaptation to Force Field and Visuomotor Perturbation. *J Neurophysiol.,* 107, 134–147.

Gao, Z., van Beugen, B.J., De Zeeuw, C.I. (2012). Distributed Synergistic Plasticity and Cerebellar Learning. *Nat Rev Neurosci*., 13, 619-35.

Garrido, J.A., Luque, N.R., D'Angelo, E., Ros, E. Distributed cerebellar plasticity implements adaptable gain control in a manipulation task: a closed-loop robotic simulation. Submitted to *Front. Neural Circuits*.

Hwang, E.J., Shadmehr, R.J. (2005). Internal Models of Limb Dynamics and The Encoding of Limb State. *Neural Eng*., 2(3), 266-78.

Hoffland, B.S., Bologna, M., Kassavetis, P., Teo, J.T.H., Rothwell, J.C., Yeo, C.H., van de Warrenburg, B.P., Edwards, M.J. (2012). Cerebellar Theta Burst Stimulation Impairs Eyeblink Classical Conditioning. *J Physiol*., 590(4), 887-897.

Ito M. (2006). Cerebellar Circuitry as a Neuronal Machine. *Prog Neurobiol.*, 78, 272–303.

Luque, N.R., Garrido, J.A., Carrillo, R.R., Coenen, O.J., Ros, E. (2011). Cerebellar Input Configuration Toward Object Model Abstraction in Manipulation Tasks. *Neural Networks, IEEE Transactions on*, 22(8), 1321-1328.

Marr, D. (1969). A Theory of Cerebellar Cortex. *J Physiol.,* 202(2), 437–470.

van der Smagt, P. (2000). Benchmarking Cerebellar Control. *Robotics and Autonomous Systems*, 32, 237-251.

Yamamoto, K., Kawato, M., Kotosaka, S., Kitazawa, S. (2007). Encoding of Movement Dynamics by Purkinje Cell Simple Spike Activity during Fast Arm Movements under Resistive and Assistive Force Field. *J Neurophysiol*., 97(2), 1588-99.

Yamazaki, T., Tanaka, S. (2007). The cerebellum as a liquid state machine. *Neural Networks*, 20(3), 290-297.